PHYSICAL REVIEW A VOLUME 45, NUMBER 7 1 APRIL 1992

Transverse optical bistability and formation of transverse structures in a sodium-filled Fabry-Pérot resonator

J. Nalik, L. M. Hoffer, G. L. Lippi, Ch. Vorgerd, and W. Lange
Institut für Angewandte Physik, Westfälische Wilhelms-Universität Münster, Corrensstrasse 2/4, D-4400 Münster, Federal Republic of Germany
(Received 30 December 1991)

We report the observation of transverse optical bistability (TOB) in a sodium-filled Fabry-Pérot resonator, pumped by circularly polarized light, nearly resonant with the D_1 line, in the presence of a buffer gas, for low vapor density. A sequence of circularly symmetric patterns, ascribable to superpositions of resonator modes, is obtained. The appearance of TOB can be explained in terms of a self-induced intensity-dependent lens formed in the medium by the interaction with the laser light. A simple model that considers the transverse diffusion of the atoms inside the cell provides predictions in good qualitative agreement with the observations.

PACS number(s): 42.65.Pc

The appearance of transverse structures in the radiation field of lasers has been the subject of ever-increasing attention in the past few years, and the understanding of these phenomena has progressed rapidly because of the experience accumulated in the previous decade on transversally homogeneous systems. Substantial progress has been recently made with the proof of the equivalence between the theoretical description for the appearance of spatially complex patterns in lasers and hydrodynamics [1]. Very successful work in this field has already been done both experimentally and theoretically [2,3], where the structures have been interpreted in terms of a few modes of the resonator. Work on passive optical systems, instead, is not as developed. Experimental investigations have either been conducted in cavityless systems [3], or in resonators with a large number of excited modes [4]. The latter studies, although well-suited for the study of optical turbulence, are too complex for a modal analysis. The reason for extending the investigations with few excited modes to passive systems is to look for general properties of pattern formation. Furthermore, passive systems offer the advantage of permitting the excitation of selected modes, thus allowing the study of the interactions under controlled conditions. Indeed, in this respect optical systems, and in particular passive ones, may prove to be more flexible than their hydrodynamical counterpart.

We report on an experiment conducted on a passive nonlinear resonator where we excite only a few modes of the empty cavity. Here we present *only* the simplest structures observed, since they can best illustrate the basic processes behind pattern formation in this optical system. Further, we discuss a simple model where we generalize the physical description of the traditional dispersive optical bistability to the spatially nonhomogeneous case, and see how the radial dependence of the nonlinearity of the medium gives rise to distinct nonlinear resonances for the different transverse modes. The predictions of this model are in good qualitative agreement with the observations.

In the experiment we use a Fabry-Pérot resonator with both mirrors having 93% reflectivity and 25 cm radius of curvature. An intracavity windowless cell (inner diameter 12 mm), heated for a length of about 4 cm, contains the sodium vapor. Typical atomic densities used are 10^{12} to 10^{13} atoms/cm^3, and a buffer gas, argon at 200 mbar, is added. We experiment with a weak longitudinal magnetic-field component ($\sim 10^{-4}$ T) and well-compensated transverse ones (residual field $< 10^{-6}$ T). A frequency-stabilized cw ring dye laser, operating in single longitudinal mode, pumps the vapor. The transverse profile of the input beam has been controlled with an adjustable intracavity aperture and the Gaussian beam has been cleaned, after passing through an optical diode and an electro-optic modulator, with a spatial filter, before reaching the resonator. The filtered beam is mode matched, with two lenses, to the empty resonator and passed through a circular polarizer. The maximum power at the resonator input was about 120 mW. The transmitted beam was detected by photodiodes and by a charge-coupled-device camera, placed about six Rayleigh lengths away from the center of the resonator, and connected to an image processing system.

We experimented on both sides of the D_1 line but restrict the discussion to the defocusing side, since a symmetry between the two sides was observed, which we interpret later. Here we report only the results obtained for *low* atomic density ($< 5\times 10^{12}$ atoms/cm^3) in the detuning range ($\Delta = \nu_L - \nu_A$, where L and A stand for laser and atoms, respectively) between -10 and -70 GHz, where dispersive effects are predominant. For the first experiments we used a confocal resonator, because of the advantage that it offers in having all the even transverse modes frequency degenerate. In this way, we can immediately see the influence of the nonlinear medium on the transverse modes. We coupled, with "bad"-mode matching, about 20% of the input power into the TEM_{10} mode [5], a few percent into the TEM_{20} mode, with the TEM_{00} still predominantly excited. In this case, we found the sequences of transverse patterns shown in Fig. 1. In the first pattern, 1(a), the TEM_{00} mode is predominant, whereas in the second pattern, 1(b), the TEM_{10} mode predominates, and in the third, 1(c), all three lowest-order modes contribute approximately in the same amount. The super-

 © 1992 The American Physical Society

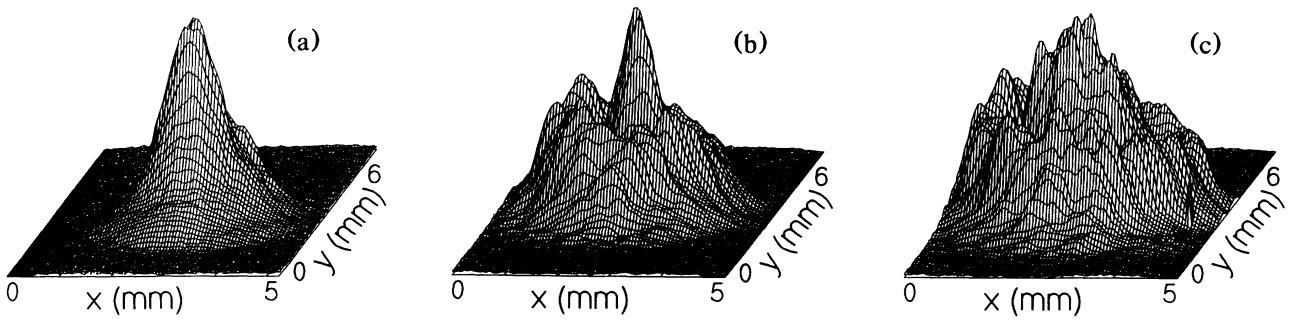

FIG. 1. Typical intensity patterns of the light transmitted by the nonlinear resonator. (a) Predominantly Gaussian mode (76% TEM_{00}, 24% TEM_{10}, $\phi = 1.7$ rad); (b) predominantly first higher-order mode (35% TEM_{00}, 65% TEM_{10}, $\phi = 1.8$ rad); (c) nearly equal contributions of first three modes (38% TEM_{00}, 35% TEM_{10}, 27% TEM_{20}, $\phi = 2.0$ rad, $\psi = 3.4$ rad). The coefficients are the result of a fit, performed on radial cuts, at the position of the camera and are given here for the intensity of the three modes. The relative phases ϕ and ψ are defined between the TEM_{10} and TEM_{00} modes, and TEM_{20} and TEM_{00} modes, respectively.

position of the modes has been determined, in amplitude and phase, by a least-squares fit on a radial cut for each of the three patterns. Multiple hysteresis curves are displayed in Fig. 2. They are obtained by scanning the input power for fixed detuning and detecting the transmitted beam near the edge of the pattern for the fundamental mode, where the sensitivity to the intensity changes with spatial distribution is particularly high [(a), (b), and (c) as in Fig. 1]. Figure 2 shows a new type of optical bistability, called transverse optical bistability (TOB), which was recently predicted [6]. Its signature is bistability between different transverse intensity distributions, not necessarily corresponding to different output powers. For low values of the sodium density ($< 5 \times 10^{12}$ atoms/cm^3) and for very careful alignment of the resonator this is the basic sequence of patterns. The last distribution appears only in a smaller parameter range, however, than the other two. For some parameter ranges we found that TOB

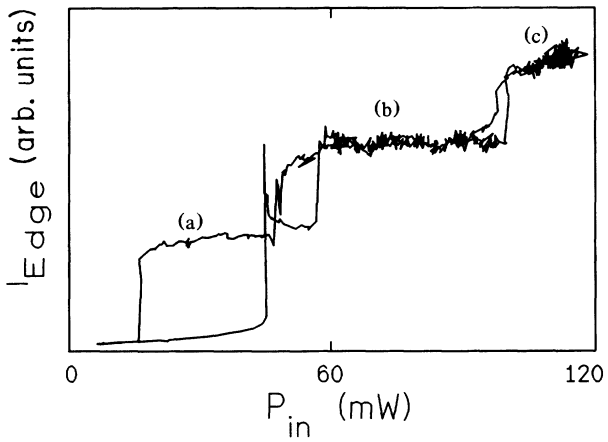

FIG. 2. Intensity measured at the output of the resonator by placing a photodiode at the edge of the pattern distribution (for the Gaussian mode) during an input power scan, for frequency detuning $\Delta = -19$ GHz and fixed cavity phase. The loops correspond to the patterns identified in Fig. 1. The overshoot, and subsequent crossing of the lines in the second hysteresis loop, are a consequence of the input power scanning speed.

was replaced by a continuous evolution of one pattern into another.

We now interpret these results on the basis of some intuitive considerations, which will be justified later in the description of the model. The interaction between the nonlinear medium and quasiresonant light having a nonhomogeneous transverse distribution causes self-focusing and self-defocusing of the incident beam [7]. The atoms, oriented by the pump beam, diffuse toward the walls of the cell, thus creating a radial gradient of orientation and therefore a gradient in the index of refraction of the medium. If we assume that this gradient may be approximated as a parabolic profile, within the laser beam cross section we have a self-induced, intensity dependent spherical lens which changes the resonance properties of the resonator. The transverse modes of the resonator experience different amounts of Gouy phase shift [8] because of this lens and their resonant frequencies are shifted one with respect to another. The generation of the patterns in Fig. 1 is thus controlled by the intracavity optical power, which determines the focal length of the lens and through it the relative shift of the resonances of the transverse modes.

These intuitive considerations can be theoretically formalized by extending a model successfully used to describe dispersive optical bistability in sodium vapor [9], specialized to our case of no transverse magnetic-field components. Indeed, we must only replace the decay of the orientation, there assumed to be exponential [9], with the diffusion of the oriented atoms away from the axis of the cell to the wall, where their orientation is destroyed.

In order to obtain an analytical solution to the diffusion problem we approximate the profile of the orientation to the lowest order of a power-series expansion, i.e., with a parabola. This approximation is not unreasonable, since it needs to be valid only in the region of interaction between the laser beam, which has a radius about 40 times smaller than that of the cell, and the medium, which fills the cell. As a matter of fact, measurements of the lensing effect performed in the same range of parameters but without resonator, have shown good qualitative agreement with the calculated dependence of the laser beam parameter on both incident power and detuning Δ. Comparison between

experimental and theoretical curves allows one to estimate the power of this spherical lens to be in the range of some tens of centimeters.

For the numerical simulations, we assume for simplicity that only two modes of the resonator are excited: the TEM_{00} and the TEM_{10}. The intracavity intensity, including interference terms between the two modes (later neglected because they do not make any qualitative changes in the predictions), is calculated at the center of the resonator, where the self-induced intensity dependent "thin lens" is assumed to be. The phase shift, different for the two modes, is explicitly calculated as a function of the (weak) lens power using *ABCD* matrix methods. The change in the finesse of the resonator due to residual absorption as a function of the vapor density and the detuning between atomic line and laser frequency is also included. Notice that in this model we use the set of modes of the nonlinear resonator to decompose a pattern. This choice is not standard and may not be generally applicable, but it offers the advantage of making the physical interpretation much more straightforward.

Figure 3(a) shows the steady-state curves of the intracavity power as a function of the resonator phase, calculated by the AUTO program [10], for negative detuning, and where about 20% of the energy is coupled into the TEM_{10} mode of the empty confocal configuration. The left-hand side peak in the figure corresponds to the nonlinear resonance of the TEM_{10} mode and the right-hand side peak to that of the TEM_{00}. This figure demonstrates how the nonlinear interaction separates the two resonances, breaking their degeneracy. Here we display the integral transmitted power contained in the TEM_{00} mode plus that in the TEM_{10} mode, with the latter contribution multiplied by a factor of two for better graphical resolution. For comparison, Fig. 3(b) shows the result of an experimental phase scan, performed at constant input power (detector near the edge of the pattern, as in Fig. 2). The steady-state curve for the output power as a function of the input power, for fixed resonator phase and under the same conditions as Fig. 3(a), is shown in Fig. 4. In the lower hysteresis loop the intensity distribution is nearly that of a TEM_{00} mode, while in the upper loop the TEM_{10} dominates, but is accompanied by a non-negligible amount of TEM_{00}. The agreement with the experimental results (Fig. 2) is quite satisfactory, since in the simulations we have not allowed for the presence of a third mode, to keep the numerics simpler.

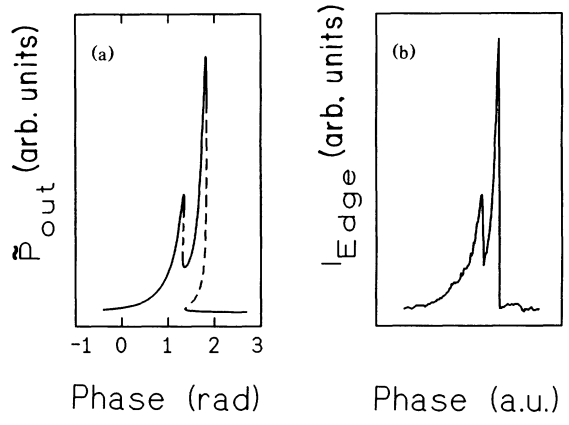

FIG. 3. (a) Steady states of the equations calculated by the AUTO program. Integrated output power $\tilde{P}=\bar{P}(TEM_{00})+2\bar{P}(TEM_{10})$ as a function of the cavity phase. The left-hand side peak shows the nonlinear resonance of the TEM_{10} mode, the right-hand side one that of the TEM_{00} mode. The dashed lines identify the unstable regions of the steady-state curve. (b) Intensity measured at the edge of the pattern (as in Fig. 2) for a cavity phase scan at constant input power. The peaks are the resonances of the patterns of Fig. 1(b) (left) and Fig. 1(a) (right).

The same calculations, when repeated for resonators that are slightly longer or shorter than confocal, predict that the parameter range in which TOB appears, for negative detuning, is broader in the shorter resonator and narrower in the longer one. Experimental measurements in nonconfocal resonators, where the deviation from the confocal cavity length amounts to about 4% in either direction, agree with this prediction. We can interpret this result by observing that the shift in the resonance frequencies introduced by the length change in the shorter resonator enhances the shift brought about by the nonlinear lens, while it inhibits this effect in the longer resonator. On the focusing side of the line the model predicts the opposite occurrence, and the experimental results agree with this prediction, although for positive detuning other effects easily take place and the range of sodium densities available for investigation is quite restricted.

In the case of very small mode mismatch ($\sim 1\%$ of the energy is coupled into the TEM_{10} mode) and low sodium density, no TOB is predicted by this model. Indeed, the mode mismatch introduced by the change in effective cavity length due to the nonlinearity alone is not large enough to generate a switch to higher-order modes. Under corresponding experimental conditions ($< 1\%$ of the energy coupled into the TEM_{10} mode and low sodium density) TOB has not been observed, in agreement with the prediction.

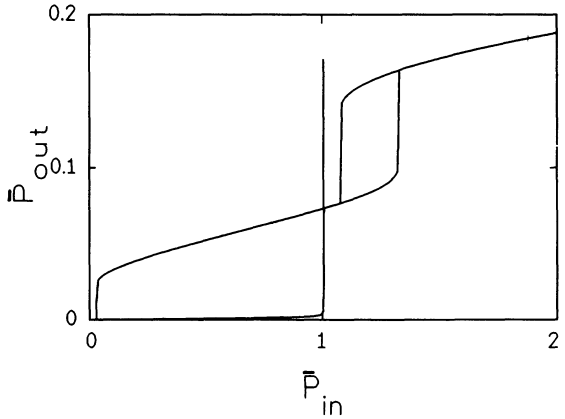

FIG. 4. The output power for a scan of the input power, from a numerical integration of the model, for comparison with Fig. 2, in units of the threshold value of the input power for the first switch. The first loop corresponds to the TEM_{00} while the second corresponds to the TEM_{10} mode with a contribution by the TEM_{00} mode.

Before concluding, we mention the observation of the following: patterns with intrinsically broken symmetry for higher sodium densities ($>5\times10^{12}$ atoms/cm^3), intensity oscillations in the Gaussian mode, periodic rotations of the asymmetric patterns, vortices, and other complex structures. Investigation of these phenomena is currently under way. A numerical study of the complete model for the nonlinear Fabry-Pérot resonator is being carried out and already provides results in good qualitative agreement with the experiment.

The authors are indebted to M. Möller for the use of his stabilization system, which made most of the measurements possible and are also very grateful for his advice on the operation of the dye laser. We would also like to thank Dr. Etrich for his help with the AUTO program. One author (L.M.H.) is grateful for the financial support from the NSF and another (G.L.L.) acknowledges the support from the Alexander von Humboldt Foundation. This work was supported by the Deutsche Forschungsgemeinschaft.

[1] M. Brambilla, L. A. Lugiato, V. Penna, F. Prati, C. Tamm, and C. O. Weiss, Phys. Rev. A **43**, 5114 (1991).

[2] Chr. Tamm, Phys. Rev. A **38**, 5960 (1988); C. Green, G. B. Mindlin, E. J. D'Angelo, H. G. Solari, and J. R. Tredicce, Phys. Rev. Lett. **65**, 3124 (1990); M. Brambilla, F. Battipede, L. A. Lugiato, V. Penna, F. Prati, C. Tamm, and C. O. Weiss, Phys. Rev. A **43**, 5090 (1991).

[3] G. Grynberg, E. Le Bihan, P. Verkerk, P. Simoneau, J. R. R. Leite, D. Bloch, S. Le Boiteux, and M. Ducloy, Opt. Commun. **67**, 363 (1988).

[4] S. A. Akhmanov, M. A. Vorontsov, and A. V. Lariekev, Kvantovaya Elektron. (Moscow) **17**, 391 (1990) [Sov. J. Quantum Electron. **20**, 325 (1990)]; F. T. Arecchi, G. Giacomelli, P. L. Ramazza, and S. Residori, Phys. Rev. Lett. **65**, 2531 (1990); A. V. Grigor'yants, and I. N. Dyuzhikov, J. Opt. Soc. Am. B **7**, 1303 (1990).

[5] Throughout this paper we always refer to Gauss-Laguerre modes.

[6] L. A. Lugiato, Wang Kaige, and N. B. Abraham (unpublished).

[7] Y. R. Shen, Prog. Quantum Electron. **4**, 1 (1975); J. H. Marburger, **4**, 35 (1975).

[8] A. E. Siegman, *Lasers* (University Science Books, Mill Valley, CA 1986).

[9] F. Mitschke, R. Deserno, W. Lange, and J. Mlynek, Phys. Rev. A **33**, 3219 (1986).

[10] Eusebius Doedel, computer code AUTO86, California Institute of Technology, Pasadena, CA, 1986.

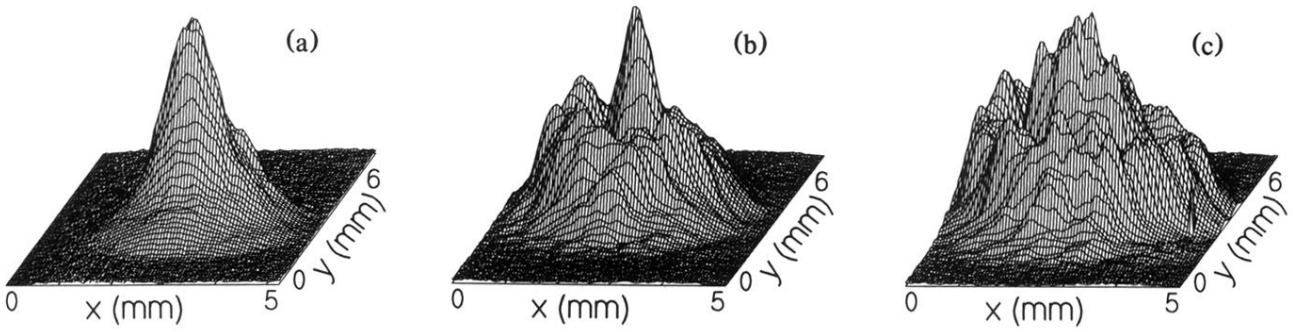

FIG. 1. Typical intensity patterns of the light transmitted by the nonlinear resonator. (a) Predominantly Gaussian mode (76% TEM_{00}, 24% TEM_{10}, $\phi = 1.7$ rad); (b) predominantly first higher-order mode (35% TEM_{00}, 65% TEM_{10}, $\phi = 1.8$ rad); (c) nearly equal contributions of first three modes (38% TEM_{00}, 35% TEM_{10}, 27% TEM_{20}, $\phi = 2.0$ rad, $\psi = 3.4$ rad). The coefficients are the result of a fit, performed on radial cuts, at the position of the camera and are given here for the intensity of the three modes. The relative phases ϕ and ψ are defined between the TEM_{10} and TEM_{00} modes, and TEM_{20} and TEM_{00} modes, respectively.